Multibody Syst Dyn (2014) 31:93–110
DOI 10.1007/s11044-013-9380-9

Calculating road input data for vehicle simulation

Michael Burger

Received: 17 January 2013 / Accepted: 11 June 2013 / Published online: 11 July 2013

Abstract Multibody system simulation is an important tool in the development process in vehicle engineering. Without much effort, different vehicle variants and designs can be simulated, analyzed, and optimized. This is of particular relevance in an early stage of development, when no physical prototypes are available yet. In order to simulate the vehicle models under realistic conditions, suitable input data is needed for the simulation. We present an approach to derive a virtual road profile based on a tire-surrogate model, measured spindle forces, and a multibody system model of the measurement vehicle. In contrast to the measured spindle forces, the road profile together with the tire-surrogate model can be used to simulate other vehicle variants, for which no measurements are available. The road profile is derived by solving an inverse control problem. We formulate this inverse problem in the context of system simulation and provide a short mathematical analysis. Additionally, we discuss a solution approach, the method of control-constraints, which is also applied in a numerical simulation study to compute a virtual road profile.

Keywords Multibody systems · Vehicle engineering · Numerical simulation · Inverse problems · Control

1 Introduction

Today, numerical system simulation plays an important role in many technical areas, especially in vehicle engineering. The design and development process of a new vehicle can be accelerated significantly by using numerical simulation methods. A simulation on a computer is efficient and results are easy to reproduce, different variants, designs, and configurations as well as different load scenarios can be simulated, analyzed, and optimized rapidly and easily [17, 28].

In the development process, the vehicle and its components have to be examined and assessed with respect to durability and fatigue under realistic conditions, it is necessary to

M. Burger (✉)
Fraunhofer Institute for Industrial Mathematics, Fraunhofer-Platz 1, 67663 Kaiserslautern, Germany
e-mail: michael.burger@itwm.fraunhofer.de

know the loads that act on the vehicle's components. The latter can be obtained by measurement during a test-track drive or on a servo-hydraulic test-rig in the laboratory. Another very efficient alternative and state-of-the-art method in automotive industry is to use numerical system simulation [16]. The vehicle is modeled as multibody system (MBS), possibly including flexible components, hydraulic elements, bearings, controllers etc., and it is simulated to obtain the relevant loads as outputs of the numerical integration [2]. This approach is especially useful in an early stage of development, in which no physical prototype is available yet, and thus it is impossible to perform test-track drives or test-rig runs while measuring the corresponding loads.

For the system simulation, it is crucial to have suitable input data, such that a numerical simulation under realistic conditions can be achieved. There are mainly three simulation scenarios that realize this task, cf. [3, 11, 12]. The first is a so-called full-vehicle simulation on a digital road. Here, a detailed MBS model of the vehicle is needed, including a model of the driver with a specified driving pattern, and a model of the tire in a suitable quality. In addition, a measured and digitized road profile must be available. All these necessary ingredients require a high modelling effort [3]. The second approach is to apply measured spindle forces and to perform a force-excited simulation. Apart from the numerical difficulties of such a simulation (see [27]), the spindle forces depend highly on the vehicle that was used for the measurement. Therefore, they can only be used to simulate a model of the specific measurement vehicle, not for other vehicle models. The third scenario consists in deriving a suitable invariant input quantity based on a vehicle model, for which measured quantities are available, e.g., the predecessor vehicle of a new design. An invariant input quantity in this context is an input quantity that is independent on the vehicle under consideration, i.e., it is invariant with respect to certain modifications of the vehicle, and thus it can be used to simulate vehicle variants, for which no prototype or measured data is available. As an example for such an invariant quantity, we propose a six-dimensional virtual road profile in connection with a tire-surrogate model [11, 12]. This virtual profile can be interpreted as the motion of a frame attached at an idealized tire contact point. Using this approach, neither a complex tire and driver model nor a digitized road is needed. However, to obtain this virtual road profile, an inverse control problem has to be solved.

From a system-theoretic point of view, this inverse control problem can be formulated as follows. Let S denote the system, for which measured quantities are available, the MBS model of a car, for example. Furthermore, let y_{REF} denote the measured quantities at the corresponding real car. Then the task is to find an input quantity u for the system S that reproduces the measured quantities:

$$y_{\mathrm{REF}} = S(u). \tag{1}$$

For the testing on servo-hydraulic test-rigs, an inverse problem of the same kind has to be solved, in order to excite the test-rig properly [14, 15]. Here, S represents the physical test-rig and a mathematical description can only be determined by methods of experimental system identification [14]. The inverse problem is then solved iteratively by inverting a linearized, experimentally estimated transfer function [15, 29]. This approach is useful, if there is not more information about the considered system available, but the difficulties are apparent: the linearization and estimation does not globally reflect the nonlinear behavior of the test-rig, convergence, and stability properties are often very poor, a high number of iterations, and expert knowledge is typically indispensable to obtain a satisfying solution [15].

If the considered system is a simulation model, however, a lot more information is available. In case of an MBS model, the mathematical description is known in terms of differential equations based on physical modeling techniques. In this paper, we only consider

systems that are numerical simulation models. We present a mathematical analysis and a solution approach, cf. also [11].

Apart from the described application case, similar inverse problems appear in the path planning and control of robots, cranes, [8, 24], and aircrafts [6, 10]. See also [30] for further examples.

The remaining part of this paper is organized as follows. In Sect. 2, we provide a short mathematical analysis. The inverse control problem is formulated and a solution approach is presented. In Sect. 3, we discuss in detail the application to vehicle simulation. We describe a procedure that allows to concentrate on tire-surrogate models, in order to derive a virtual road profile. In a numerical case study, we analyze the invariance properties of the computed input data. After that, a concluding discussion follows in Sect. 4.

2 Mathematical analysis of the inverse control problem

In this section, we provide a mathematical framework, in order to formulate precisely an inverse control problem in the context of system simulation. In addition, we present a short analysis of that problem. Throughout this section, we assume that the appearing right-hand side and output functions f, g, k, h are sufficiently smooth and that the corresponding initial-value problems possess a unique solution existing on the considered time intervals.

2.1 Formulation of the inverse control problem

We consider a general dynamical system mathematically described as nonlinear first-order ordinary differential equation (ODE) of the form

$$\dot{x} = f(t, x, u), \tag{2}$$

with $x \in \mathbb{R}^{n_x}$ called the state of the system and u the input or control. Obviously, the equations of motion of a controlled mechanical MBS [17],

$$M(q)\ddot{q} = k(t, q, \dot{q}, u), \tag{3}$$

with position coordinates $q \in \mathbb{R}^{n_q}$, the mass matrix $M \in \mathbb{R}^{n_q \times n_q}$ and k subsuming all acting forces, can be seen as a special case of this general form. Indeed, by transforming into a first-order system,

$$\begin{aligned} \dot{q} &= v, \\ \dot{v} &= M(q)^{-1} k(t, q, v, u), \end{aligned} \tag{4}$$

and by setting $x = (q^T, v^T)^T \in \mathbb{R}^{2n_q}$ and $f(t, x, u) := (v^T, k(t, q, v, u)^T)^T$, we obtain the form given in (2).

Numerical system simulation in this context means the numerical solution of the initial value problem (IVP) given by (2) on a given time interval $I := [0; T]$, $T > 0$ and the condition

$$x(0) = x_0 \tag{5}$$

with a given vector $x_0 \in \mathbb{R}^{n_x}$ and a given input function u, cf. [2, 17].

Next, we define the system-outputs,

$$y(t) := h\big(t, x(t), u(t)\big) \tag{6}$$

for $t \in [0; T]$ and an output function $h : I \times \mathbb{R}^{n_x} \times \mathbb{R}^{n_u} \to \mathbb{R}^{n_y}$. We remark that in most application scenarios, the output function h is not explicitly depending on the control, i.e., $h_u \equiv 0$. If, however, the acceleration of a controlled body is considered as output, an explicit dependency may occur. Thus, for sake of completeness, we consider the general case in the sequel.

In a functional view, system simulation can be described by the solution operator, [11], which we define for the initial value problem (2), (5) as follows:

$$\begin{aligned} \mathcal{F} : L^\infty\big(I; \mathbb{R}^{n_u}\big) &\longrightarrow W^{1,\infty}\big(I; \mathbb{R}^{n_x}\big), \\ u \quad &\mapsto \text{ corresponding solution of the IVP (2), (5).} \end{aligned} \tag{7}$$

$L^\infty(I; \mathbb{R}^{n_u})$ denotes the space of essentially bounded functions and $W^{1,\infty}(I; \mathbb{R}^{n_x})$ is the space of absolutely continuous function with essentially bounded first derivative. Moreover, the *input–output-operator* is defined as

$$\begin{aligned} \mathcal{F}_h : L^\infty\big(I; \mathbb{R}^{n_u}\big) &\longrightarrow L^\infty\big(I; \mathbb{R}^{n_y}\big), \\ u \quad &\mapsto \mathcal{F}_h(u), \end{aligned} \tag{8}$$

with

$$\big[\mathcal{F}_h(u)\big](t) := h\big(t, \big[\mathcal{F}(u)\big](t), u(t)\big), \quad t \in I. \tag{9}$$

That is, a given input or control function u is mapped to the output, a function of the solution of the corresponding IVP (2), (5), and possibly the input itself. Computing the output for a given input is the task of classical system simulation, it is also called the forward (simulation) problem.

In contrast, the scenario discussed in the introduction leads to the corresponding inverse (or backward) problem. Indeed, the so-called reference outputs are given by measurement data, as functions of time,

$$y_{\mathrm{REF}} : I \longrightarrow \mathbb{R}^{n_y}, \tag{10}$$

and for a given system, we search for an input function u that reproduces these measured reference trajectories as simulation outputs. In particular, it is the task to derive an input $u \in L^\infty(I; \mathbb{R}^{n_u})$, such that

$$\mathcal{F}_h(u) \stackrel{!}{=} y_{\mathrm{REF}}. \tag{11}$$

We call this problem the *inverse control problem* since, in fact, an inversion of the input–output-operator is required. In literature, problems of this kind are also known as tracking problems, cf. [26]. A generalization is the problem to find u such that

$$\big\|\mathcal{F}_h(u) - y_{\mathrm{REF}}\big\| \longrightarrow \min, \tag{12}$$

with a suitable norm. Such problems are called optimal control problems—for an overview and discussion, we refer to [11].

2.2 Solving the inverse control problem

In the sequel, we describe a solution approach for the previously formulated inverse control problem. In this paper, we restrict our considerations to the case that the number of inputs equals the number of outputs, i.e., $n_u = n_y =: n$. Moreover, we assume for our analysis that the reference outputs y_{REF} are smooth functions, which can be achieved by means of interpolation provided that the sampling frequency of the measured data is sufficient.

To invert the input–output-operator and, thereby, to solve the inverse control problem given in (11), we consider the following differential-algebraic equation (DAE):

$$\dot{x} = f(t, x, u) \tag{13}$$

$$0 = h(t, x, u) - y_{\mathrm{REF}}(t), \tag{14}$$

with the differential variable $x \in \mathbb{R}^{n_x}$ and the algebraic variable $u \in \mathbb{R}^{n_u}$. The strategy here is to add Eq. (14) as algebraic equation to the original system equation (13), in order to enforce the requirement of the inverse control problem for all $t \in I$. Consequently, the (unknown) input u is considered as algebraic variable in the DAE system (13)–(14) corresponding to the algebraic equation. The latter is also called control-constraint [6, 23], servo-constraint [7] or path-constraint [10]. A number of variants of this approach can be found in literature; we refer to [5–9, 24, 25] and also to our work in [11]. Together with the initial condition,

$$\left(x^T, u^T\right)^T = \left(x_0^T, u_0^T\right)^T, \tag{15}$$

Eqs. (13)–(15) constitute a DAE initial value problem. The initial value $u_0 \in \mathbb{R}^{n_u}$ has to be determined such that $(x_0^T, u_0^T)^T$ is a consistent initial value, where consistency is meant in the sense of classical DAE theory, cf. [10, 21].

If there exists a solution $(x, u) \in W^{1,\infty}(I; \mathbb{R}^{n_x}) \times L^\infty(I; \mathbb{R}^{n_u})$, the corresponding u is obviously a solution of the inverse control problem. Whence, if we assume that for each $y_{\mathrm{REF}} \in L^\infty(I; \mathbb{R}^{n_y})$, there is a unique solution of the IVP (13)–(15) on I, then the solution operator

$$\begin{aligned} \mathcal{G} : L^\infty\left(I; \mathbb{R}^{n_y}\right) &\longrightarrow L^\infty\left(I; \mathbb{R}^{n_u}\right) \\ y_{\mathrm{REF}} &\mapsto u, \text{ where } (x, u) \text{ is the solution of the IVP (13)–(15)} \end{aligned} \tag{16}$$

is the inverse of the input–output-operator, $\mathcal{G} = \mathcal{F}_h^{-1}$. To compute a solution numerically, the DAE IVP can be solved by a suitable integration scheme for DAEs; see, e.g., [10, 20, 21]. We call this approach to solve the inverse control problem the *method of control-constraints*.

The index of a DAE The index of a DAE is a well-known concept to classify DAEs [13, 19, 21]. It can be seen as a measure of the regularity of the DAE: the higher the index, the more sensitive is the solution of the DAE to perturbations, this can lead to severe problems in the numerical treatment of higher index DAEs [20]. For DAEs of the form (13)–(14), the (differentiation) index is defined to be the smallest number ν such that

$$0 = \frac{d^\nu}{dt^\nu}\left[h(t, x, u) - y_{\mathrm{REF}}(t)\right] \tag{17}$$

can be transformed into an ODE for u only using algebraic manipulations and (13), provided that y_{REF} is sufficiently smooth. For instance, if the Jacobian $h_u = \partial h / \partial u(t, x, u)$ is

nonsingular for all (t, x, u), then the index equals one. Indeed, formally differentiating leads to

$$0 = \frac{d}{dt}\big[h(t,x,u) - y_{\mathrm{REF}}(t)\big] = h_t(t,x,u) + (h_x f)(t,x,u) + h_u \dot{u} - \dot{y}_{\mathrm{REF}}(t), \tag{18}$$

and this equation can be solved for $\dot{u}$ provided that h_u is nonsingular. The effect of a high index is illustrated, when we assume that we have to deal with measurement errors, i.e.,

$$\hat{y}_{\mathrm{REF}}(t) = y_{\mathrm{REF}}(t) + \Delta y(t), \tag{19}$$

with a perturbation Δ. If the DAE (13)–(14) has index $\nu \geq 1$, then there is a constant $c > 0$ independent of Δ such that

$$\big\|u(t) - \hat{u}(t)\big\| \leq c \cdot \Big(\max_{s\in I}\big\|\Delta(s)\big\| + \cdots + \max_{s\in I}\big\|\Delta^{(\nu-1)}(s)\big\|\Big), \tag{20}$$

whenever the right-hand side is sufficiently small, [21], and u denotes the unperturbed solution. This is especially problematic if Δ is a high-frequent perturbation.

Apart from the previously mentioned assumption that the number of inputs equals the number of outputs, $n_u = n_y$, there are no further restrictions on the dimensions in this solution approach. In particular, both underactuated systems with $2n_u < n_x$ as well as fully actuated and also overactuated systems with $2n_u = n_x$ and $2n_u > n_x$, respectively, are possible.

2.2.1 Force-chains

In the remaining part of this section, we provide an analysis of the method of control-constraints when applied to a certain class of MBS. In the previous discussion, we have considered general dynamical system of the form given in Eq. (2), whereas we specialize now to the MBS equations of motion for a system with N bodies, which are only linked by force-elements, i.e., $q = (q_1^T, \ldots, q_N^T)^T \in \mathbb{R}^{Nn_q}$, $n_q = 6$ and we consider equations of the form

$$\begin{aligned} \dot{q} &= v, \\ \begin{bmatrix} M_1(q_1) & & & \\ & M_2(q_2) & & \\ & & \ddots & \\ & & & M_N(q_N) \end{bmatrix} \begin{bmatrix} \dot{v}_1 \\ \dot{v}_2 \\ \vdots \\ \dot{v}_N \end{bmatrix} &= \begin{bmatrix} f_1(q,v) \\ f_2(q,v) \\ \vdots \\ f_N(q,v) \end{bmatrix} + B(q)u. \end{aligned} \tag{21}$$

Moreover, we assume that the force vector $f = (f_1, \ldots, f_N)$ describes a force-chain between body 1 and body N, i.e., by definition,

$$\begin{aligned} f_1 &= f_1(q_1, v_1, q_2, v_2), \\ f_j &= f_j(q_{j-1}, v_{j-1}, q_j, v_j, q_{j+1}, v_{j+1}), \quad (2 \leq j \leq N-1), \\ f_N &= f_N(q_{N-1}, v_{N-1}, q_N, v_N). \end{aligned} \tag{22}$$

We set

$$J_{ij}^q := M_i^{-1} \frac{\partial f_i}{\partial q_j} \in \mathbb{R}^{n_q \times n_q}, \qquad J_{ij}^v := M_i^{-1} \frac{\partial f_i}{\partial v_j} \in \mathbb{R}^{n_q \times n_q}, \tag{23}$$

for $i, j = 1, \ldots, N$ and the input is assumed to only act on the first body,

$$B(q) = \left[b_1(q)^T, 0, \ldots, 0\right]^T \in \mathbb{R}^{Nn_q \times n_u}, \tag{24}$$

with $b_1(q) \in \mathbb{R}^{n_q \times n_u}$. We consider an output function of the form

$$h(q, v) := H_N(q) M_N(q)^{-1} f_N(q, v), \tag{25}$$

with a given matrix function $H_N(q) \in \mathbb{R}^{n_y \times n_q}$, i.e., the output is a part of the acceleration of the Nth body, we do not require that $n_y = n_q$. Applying the method of control-constraints means adding the algebraic equation,

$$0 = H_N(q) M_N(q)^{-1} f_N(q, v) - y_{\mathrm{REF}}(t) \tag{26}$$

to (21). We prove the following theorem, cf. [11].

Theorem 1 *For the index k of the DAE system (21)–(26), we have*:

(a)

$$k \geq N, \tag{27}$$

(b) $k = N$, *if the matrix*

$$\Sigma := H_N J^v_{N,N-1} J^v_{N-1,N-2} \cdots J^v_{2,1} b_1 \tag{28}$$

is nonsingular for all $q, v \in \mathbb{R}^{N \cdot n_q}$.

(c) *If Σ as defined above is singular, but replacing in its definition L Jacobian matrices J^v_{ij} by their position counterparts J^q_{ij} makes the matrix product in (28) nonsingular, then*

$$k \leq N + L. \tag{29}$$

Proof To prove these statements, we only need to observe that for $j \in \{1, \ldots, N-1\}$ and a function

$$\varphi = \varphi(q_j, v_j, q_{j+1}, v_{j+1}, \ldots, q_N, v_N) \tag{30}$$

not depending on q_l, v_l, $(1 \leq l \leq j-1)$ and u, we have

$$\frac{d^j}{dt^j}\left[\varphi(q_j, v_j, q_{j+1}, v_{j+1}, \ldots, q_N, v_N)\right] = \left(\varphi_{v_j} J^v_{j,j-1} \cdots J^v_{2,1} b_1\right)(q, v)u + \Pi(q, v), \tag{31}$$

where the function Π does not depend on u and, additionally that

$$\frac{d^l}{dt^l}\varphi(q_j, v_j, q_{j+1}, v_{j+1}, \ldots, q_N, v_N) \tag{32}$$

does not depend on u for $l \leq j-1$. This is shown by a simple inductive argument and proves (a) and (b) by taking $j = N-1$ and

$$\varphi(q_{N-1}, v_{N-1}, q_N, v_N) := H_N(q_N) M_N^{-1}(q_N) f_N(q_{N-1}, v_{N-1}, q_N, v_N). \tag{33}$$

In addition, if the assumption of (c) holds, after at most $N - 1 + L$ differentiation steps, we may solve for u. □

Fig. 1 Force-chain

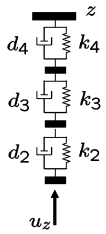

If the output is depending only on the position of the last body, the index would be increased at least by two when compared to the considered acceleration case, since one needs at least two time differentiation steps to be on acceleration level. Accordingly, if the output only depends on the velocity of the last body, the index would be increased at least by one.

Example The one-dimensional N-mass-spring-damper system for $N = 4$, is a very simple example of a force chain: the spring-damper elements connect the bodies 1 (bottom) to 4 (top), the input acts as a force on the first body at the bottom and as output, the acceleration of the highest body is considered, cf. Fig. 1. Let us study the system in more detail: assume that all four bodies have unit mass and are only allowed to move in vertical direction, let denote $q_j, v_j \in \mathbb{R}$, $(1 \leq j \leq 4)$ their vertical displacements and velocities. If the spring-damper elements between the bodies are described by linear force-laws, the components of the force vector are given by

$$\begin{aligned} f_4 &= -k_4 \cdot (q_4 - q_3) - d_4 \cdot (v_4 - v_3) + c_4, \\ f_j &= -k_j \cdot (q_j - q_{j-1}) - d_j \cdot (v_j - v_{j-1}) + k_{j+1} \cdot (q_{j+1} - q_{j1}) - d_{j+1} \cdot (v_{j+1} - v_j) \\ &\quad + c_j, \quad (j = 2, 3), \\ f_1 &= k_2 \cdot (q_2 - q_1) + d_2 \cdot (v_2 - v_1) + c_1 + u_z, \end{aligned} \tag{34}$$

where c_j, $(j = 1, \ldots, 4)$ are some real constants (such as gravity and rest lengths), and k_j denote the stiffness-coefficients and d_j denote damping-coefficients with $(k_j, d_j) \neq (0, 0)$ for $j = 2, \ldots, 4$. Then, choosing $H_4 = 1$, the matrix Σ from (28) reads as

$$\Sigma = d_4 \cdot d_3 \cdot d_2. \tag{35}$$

Consequently, if $d_i \neq 0$ for all $i = 2, \ldots, 4$, the index of the DAE system is 4. If we have for only one $i \in \{2, \ldots, 4\}$ $d_i = 0$, i.e., actually, no damper, then the index increases by one. Therefore, the number L of (29) may be interpreted as the number of *missing* dampers. A similar case study can be found in [4].

Theorem 1 and the preceding example show that the index of the DAE system may increase *linearly* with the number of bodies between the body at which the control acts and the body at which the output is measured, provided that force-elements are between the involved bodies. Roughly speaking, if there are only force-elements between the bodies of a MBS, we have as a rule of thumb: the larger the distance is between input and output, the higher the index of the corresponding DAE system might be. Without giving a precise definition, distance means here, of course, the number of bodies in between.

Concerning the computational applicability, this results constitutes a severe drawback of the presented approach to invert the input–output operator, since in realistic MBS the

distance between input and output is often more than two bodies. The previously discussed example underlines this aspect: even for a simple one-dimensional four-mass-spring-damper system as considered therein, the index of the corresponding augmented DAE system is at least 4, for an analog three-mass-spring-damper systems it is still at least 3.

The purpose of the preceding theorem and the discussion is to give some insights in the method of control constraints and to underline also its drawbacks. DAE problems of an index up to three may be solved numerically in a robust and reliable way, whence, the distance in the previous sense must not be too large.

In case of a differentially flat system [18], the input (as well as the states) can be expressed in terms of the desired output and its time-derivatives. Obviously, this would directly solve the inverse control problem. Nevertheless, for large and complex systems the derivation of these expressions may be very costly and time-consuming, if not practically impossible. Thus, also for theses systems, the method of control-constraints may be helpful, cf. also the comments in [25].

3 Application to full vehicle simulation

3.1 Preliminary discussion

In this section, we come back to the motivating application scenario presented in the Introduction, Sect. 1. The aim is to back-calculate an invariant input quantity from measured data of a reference vehicle and a corresponding (three-dimensional) MBS model of that vehicle, which is built up in the commercial MBS software tool ADAMS [1].

In what follows, we describe an approach to solve this task, cf. [11, 12]. We introduce a specific six-dimensional tire-surrogate model, which has a six-dimensional, virtual road profile as input—three quantities for the translational degrees of freedom and three quantities correspond to the rotational degrees of freedom. The virtual profile can be interpreted as the motion of a frame attached to an idealized contact point of the tire-surrogate model. The latter is coupled to each of the four rims of the vehicle model. Then, by solving an inverse control problem, four virtual road profiles are derived that reproduce the measurement data for the reference vehicle.

After this step, the *pairs* consisting of the tire-surrogate models and the corresponding derived profiles are considered as excitation model, which possesses a certain invariance property, and thus it can be used to simulate models of other variants different from the reference vehicle. Moreover, the specific structure of the interface between tire and vehicle model (see Fig. 2) allows to solve the inverse control problem only for the tire-surrogate models instead of the coupled system.

To achieve this, a two-step procedure is necessary, which we describe in the framework of general dynamical systems in state-space form.

Two-step procedure Let $f_A : [0; T] \times \mathbb{R}^{n_A} \times \mathbb{R}^{n_v} \to \mathbb{R}^{n_A}$, $f_B : [0; T] \times \mathbb{R}^{n_A} \times \mathbb{R}^{n_B} \to \mathbb{R}^{n_B}$ and $\mathcal{V} : \mathbb{R}^{n_A} \times \mathbb{R}^{n_B} \to \mathbb{R}^{n_v}$ denote smooth right-hand side and output functions such that the solution-operators for the corresponding IVPs are well-defined on $L^\infty := L([0; T]; \mathbb{R}^{n_u})$. Then we consider the three systems A, B, and the combined system AB:

1. System A, $S_A := (L^\infty, \mathcal{F}^A)$:

$$\begin{aligned} \dot{x}_A(t) &= f_A\big(t, x_A(t), v(t)\big), \\ x_A(0) &= x_{A,0}. \end{aligned} \tag{36}$$

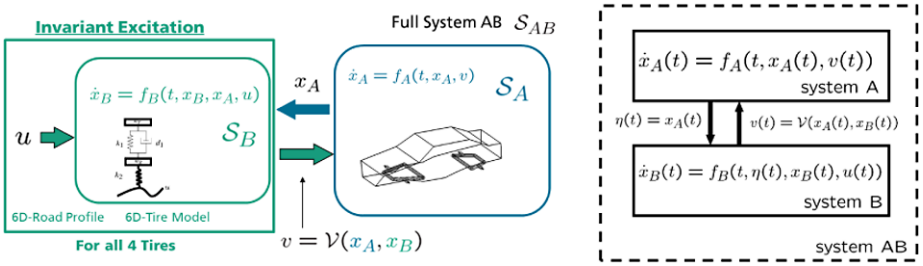

Fig. 2 The interface between vehicle and tire model

Whence, for $v \in L^\infty$, $\mathcal{F}^A(v) = x_A$. This system will correspond to the vehicle model.

2. System B, $S_B^\eta = (L^\infty, \mathcal{F}^{B,\eta})$, it depends additionally on a given time dependent function $\eta : [0; T] \to \mathbb{R}^{n_A}$:

$$\begin{aligned} \dot{x}_B(t) &= f_B\big(t, \eta(t), x_B(t), u(t)\big) \\ &=: f_B^\eta\big(t, x_B(t), u(t)\big), \\ x_B(0) &= x_{B,0}. \end{aligned} \tag{37}$$

Whence, for $u \in L^\infty$, $\mathcal{F}^{B,\eta}(u) = x_B$. Here, we consider the output function $h_B(t, x_B) := \mathcal{V}(\eta(t), x_B)$. This system will correspond to the four tire-surrogate models.

3. System $S_{AB} = (L^\infty, \mathcal{F}^{AB})$:

$$\begin{aligned} \dot{x}_{AB,A}(t) &= f_A\big(t, x_{AB,A}(t), \mathcal{V}\big(x_{AB,A}(t), x_{AB,B}(t)\big)\big), \\ \dot{x}_{AB,B}(t) &= f_B\big(t, x_{AB,A}(t), x_{AB,B}(t), u(t)\big), \\ \big(x_{AB,A}(0), x_{AB,B}(0)\big) &= (x_{AB,A0}, x_{AB,B0}). \end{aligned} \tag{38}$$

Whence, for $u \in L^\infty$, $\mathcal{F}^{AB}(u) = (x_{AB,A}, x_{AB,B})$. We define the output function $h_{AB}(t, x_{AB,A}, x_{AB,B}) := \mathcal{V}(x_{AB,A}, x_{AB,B})$, $\mathcal{F}_{h_{AB}}^{AB}$ denotes the corresponding input–output-operator. This system corresponds to the coupled system vehicle and tire-surrogate models.

The two-step procedure is given as follows:

1. First, we consider the subsystem A with input v_{REF} and the corresponding solution $x_A = \mathcal{F}^A(v_{\mathrm{REF}})$.
2. Second, we consider the subsystem B with the choice $\eta = x_A = \mathcal{F}^A(v_{\mathrm{REF}})$ and derive the input u that solves the inverse control problem

$$\mathcal{F}_{h_B}^{B,x_A}(u) = v_{\mathrm{REF}} \quad \Leftrightarrow \quad \mathcal{V}\big(x_A(t), x_B(t)\big) = v_{\mathrm{REF}}(t), \quad t \in [0; T], \tag{39}$$

with $x_B = \mathcal{F}^{B,x_A}(u)$. This is done by the method of control-constraints, described in Sect. 2. The corresponding inverse control problem *only involves* the subsystem B.

Theorem 2 *For the input u derived by the above two-step procedure, it holds*

$$\mathcal{F}_{h_{AB}}^{AB}(u) = v_{\mathrm{REF}} \quad \Leftrightarrow \quad \mathcal{V}\big(x_A(t), x_B(t)\big) = v_{\mathrm{REF}}(t), \quad t \in [0; T], \tag{40}$$

with $(x_A, x_B) = \mathcal{F}^{AB}(u)$. In words, if the combined system AB is solved with the input u, then the corresponding output equals the desired reference.

Proof Following the described two-step procedure, let $x_A := \mathcal{F}^A(v_{\mathrm{REF}})$, let u satisfy $\mathcal{F}_{h_B}^{B,x_A}(u) = v_{\mathrm{REF}}$ and denote $x_B := \mathcal{F}_B^{x_A}(u)$. Then we write the combined system:

$$\dot{x}_{AB,A}(t) = f_A\big(t, x_{AB,A}(t), \mathcal{V}\big(x_{AB,A}(t), x_{AB,B}(t)\big)\big), \tag{41}$$

$$\dot{x}_{AB,B}(t) = f_B\big(t, x_{AB,A}(t), x_{AB,B}(t), u(t)\big), \tag{42}$$

$$\big(x_{AB,A}(0), x_{AB,B}(0)\big) = (x_{A,0}, x_{B,0}). \tag{43}$$

The pair $(x_{AB,A}, x_{AB,B}) := (x_A, x_B)$ satisfies Eq. (42) and $\mathcal{V}(x_A, x_B) = v_{\mathrm{REF}}$ by the definition of x_B and u as solution of the inverse control problem. Whence, the pair also satisfies Eq. (41) by the definition of x_A. Consequently, $(x_{AB,A}, x_{AB,B}) = (x_A, x_B)$ is the unique solution of the combined system. □

Application to the vehicle model

Coming back to the vehicle simulation, the first step means a (stabilized) force-excited simulation of the MBS model of the reference vehicle with the measured spindle forces and torques as input, we have

$$v_{\mathrm{REF}} = \big(v_{\mathrm{REF},1}^T, v_{\mathrm{REF},2}^T, v_{\mathrm{REF},3}^T, v_{\mathrm{REF},4}^T\big)^T \in \mathbb{R}^{4\cdot 6}, \tag{44}$$

with $v_{\mathrm{REF},j} \in \mathbb{R}^6$ being measured forces and torques acting on spindle j, $j = 1, \ldots, 4$. We point out that these spindle forces and torques highly depend on the vehicle that was used for the measurement, whence, in general, they are not invariant. Accordingly, the interface function $\mathcal{V}$ describes the force and torques that are produced by the tire-surrogate model.

As tire-surrogate model, we choose a six-dimensional, linear spring-damper system. The six dimensions correspond to the six degrees of freedom of a rigid body. Consequently, for one tire-surrogate model, $j \in \{1, \ldots, 4\}$, the equations of motion have the form

$$\begin{aligned} \dot{q}_{B,j} &= v_{B,j}, \\ M_j \dot{v}_{B,j} &= K_B(q_{R,j} - q_{B_j}) + D_B(v_{R,j} - v_{B,j}) - K_U(q_{B,j} - u_j), \end{aligned} \tag{45}$$

with $x_{B,j} := (q_{B,j}, v_{q,j}) \in \mathbb{R}^{12}$ denoting the state variable of the tire-surrogate model and $M_j, K_B, K, D_B \in \mathbb{R}^{6\times 6}$ are diagonal and constant mass-, stiffness- and damping-matrices. $q_{R,j}, v_{R,j} \in \mathbb{R}^6$ are part of the vector x_A and shall denote position and velocity of the vehicle's spindles. Thus, they are given as functions of time by the first step of our procedure. The input $u_j \in \mathbb{R}^6$ is a six-dimensional virtual road profile. The interface functions $\mathcal{V}_j$ also describes a linear spring-damper element defined by K_B, D_B:

$$\begin{aligned} h(t, x, u) &:= \mathcal{V}_j(t, q_{B,j}, v_{B,j}) \\ &:= -K_B\big(q_{R,j}(t) - q_{B_j}\big) - D_B\big(v_{R,j}(t) - v_{B,j}\big) + \tilde{M}_j \ddot{q}_{R,j}(t). \end{aligned} \tag{46}$$

We consider each tire-surrogate model independently. That is, for each $j = 1, \ldots, 4$ we solve an inverse control problem consisting of the system equations (45) and the control-constraint

$$0 = \mathcal{V}_j(t, q_{B,j}, v_{B,j}) - v_{\mathrm{REF},j}(t). \tag{47}$$

Consequently, we have for each tire-surrogate model $n_x = 12$ and $n_u = n_y = 6$. The index of the corresponding DAE is 2, it can be seen as one-body force-chain with output on velocity level, cf. Sect. 2.2.

The numerical values for the parameters of this rather simple surrogate model can be obtained by experience, heuristics as well as from experiments with a real tire or a more detailed tire model.

3.2 Numerical results

In this subsection, we illustrate the previous considerations and statements with numerical results. The first step is the verification of the general approach, i.e., we will show that statement of Theorem 2 holds in the explained scenario. In a second step, we address the question of invariance and show that the pair (u, B) indeed provides an invariant input system with a certain quality. We refer also to our work in [11, 12].

For our simulations, the MBS vehicle model, i.e., system A, up to the spindles, but without tires is built in the commercial MBS software tool ADAMS [1] and is called *VehicleRef*. The tire-surrogate models are implemented in Matlab/Simulink [22]. The inverse control problem, i.e., the DAE IVP resulting from the method of control-constraints is solved numerically with the DAE integrator RADAU5; see [20, 21]. The Matlab/Simulink models of the tire-surrogates are incorporated into ADAMS with the ADAMS/Controls interface realizing the described interface between the system B and A and resulting in the combined system AB within ADAMS. The coupling scenario of this example system is depicted in Fig. 3b: A spring-damper system as simplified tire model is coupled to the vehicle model. The combined system is simulated with the computed inputs $u = (u_1^T, u_2^T, u_3^T, u_4^T)^T$, $u_j \in \mathbb{R}^6$. For all simulations, we take $T = 10\,[s]$ as the length of the considered time interval.

For the numerical simulation results, we do not use real measured wheel forces and torques, but we perform a so-called *virtual measurement* instead: The vehicle MBS model is attached with a detailed and complex tire-model and is driven over a digital road. The vertical profile of this digital road is displayed in Fig. 3a (red curve, mean-value subtracted). Concerning computation times, a virtual measurement simulation on a standard desktop PC leads to a real time factor of approximately 140.

The vehicle is accelerated to a desired velocity by a controller that applies a torque on the rear wheels; after the desired velocity is reached, it is kept constant. As an outcome of this first simulation, we obtain the wheel forces and torques $v_{\mathrm{REF},j}$, $j = 1, \ldots, 4$ from the complex tire model and consider them as measured. Simultaneously, we obtain in the same step the results for

$$x_A = \mathcal{F}^A(v_{\mathrm{REF},1}, v_{\mathrm{REF},2}, v_{\mathrm{REF},3}, v_{\mathrm{REF},4}), \tag{48}$$

where the solution-operator $\mathcal{F}^A$ is realized in this case by the ADAMS-solver algorithms. Of course, in industrial practice, both a realistic and reasonable digital road and a detailed tire model of high quality are typically not available as discussed in the Introduction, but for our verification purposes, this way provides a possibility to exclude undesired measurement influences and to avoid the drift-effect in a force-excited simulation.

In Fig. 4, the computed input $u_1 : [0; 10] \to \mathbb{R}^6$ is shown, exemplarily as outcome of the solution of the corresponding inverse control problem for the system wheel *front left*. It is important to point out that we have here a six-dimensional profile; it is a virtual and effective profile, but it does not correspond directly to the real physical profile. However, parts of the profile, namely the vertical component can be interpreted as vertical profile and can be compared to the real profile from the (virtual) measurement. This is done in Fig. 3a: The blue curve is given by $\{(u_x(t), u_z(t)) \mid t \in [0; T]\}$, the mean-value has been subtracted. Both profiles coincide very well in their characteristics and frequencies, nevertheless, they are not identical; this is due to the fact that we have used a simplified tire-surrogate model

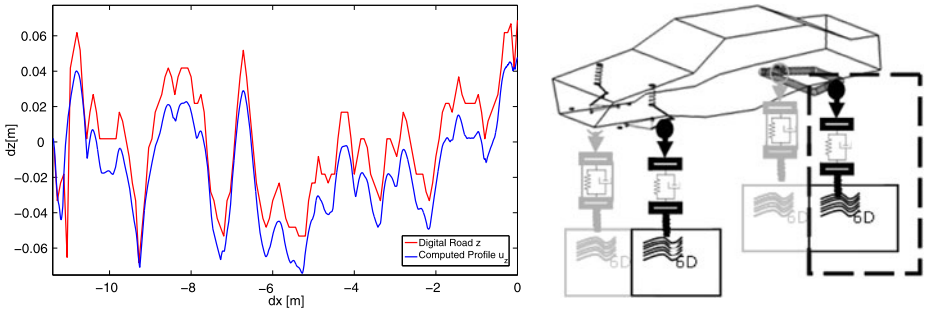

(a) Road Profiles

(b) Vehicle and Tire-Surrogate Models

Fig. 3 Road Profiles and Example System (Color figure online)

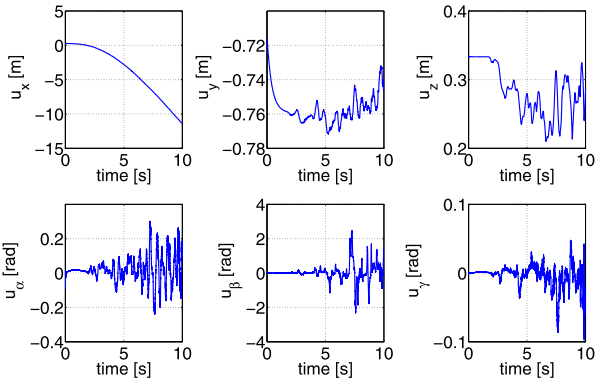

Fig. 4 Input *front left*, computed with the method of control-constraints

for the derivation. In addition, the tire-surrogate model also needs all six components of the effective profile as input, otherwise it is not working as desired.

After this, the complex tire models are removed and the vehicle is coupled at each wheel to our tire-surrogate model, cf. Fig. 3b, and it is simulated with the corresponding computed virtual road profiles. The computation time leads here to a real time factor of about 45. The outputs of this simulation are the six wheel forces and torques that are generated by each of the tire-surrogate models. For the *front left* wheel, the latter are plotted in Fig. 5 together with the corresponding reference signals $v_{\mathrm{REF},1}$. We can observe that both curves coincide very well.

3.3 Invariance

In order to check the invariance property of the proposed input system (u, B), we have to couple it to several variants of the system A, that is, to several variants of the vehicle MBS model. To this end, we define a class of three more vehicle variants attached with reference signals, which we obtained as before by a virtual measurement with the corresponding vehicle variant, cf. [11]:

$$\mathcal{C} := \big\{(\mathit{VehicleVar}1, v1_{\mathrm{REF}}), (\mathit{VehicleVar}2, v2_{\mathrm{REF}}), (\mathit{VehicleVar}3, v3_{\mathrm{REF}})\big\}. \tag{49}$$

The vehicle variants are defined as follows:

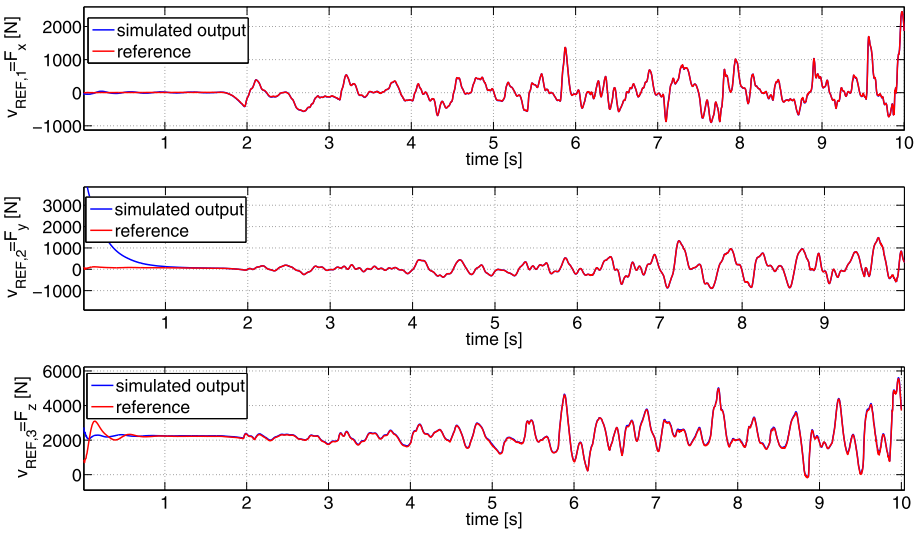

(a) Wheel Forces, front left

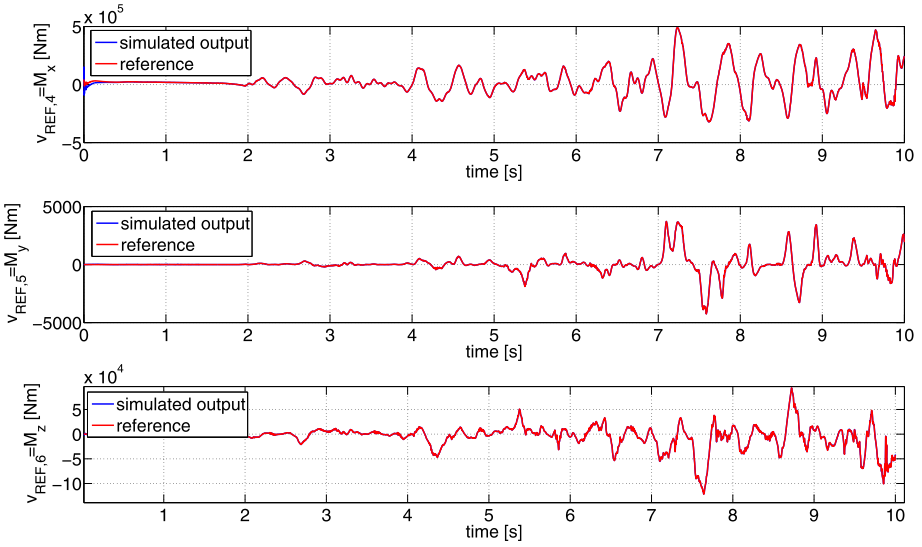

(b) Wheel Torques, front left

Fig. 5 Wheel forces and torques: simulation and reference

– VehicleVar1: Increasing of chassis mass by 100 [kg],
– VehicleVar2: Increasing of suspension stiffness coefficients by 50 %,
– VehicleVar3: Decreasing of suspension stiffness coefficients by 30 %.

All relative statements refer to system A (= VehicleRef). The computation times for the variants are in the same range as for the reference vehicle. The obtained simulation results are displayed in Figs. 6, 7 and 8. As expected, owing to the simple tire-surrogate model, the curves do not coincide as well as before. Nevertheless, the correlation is still of a remarkable

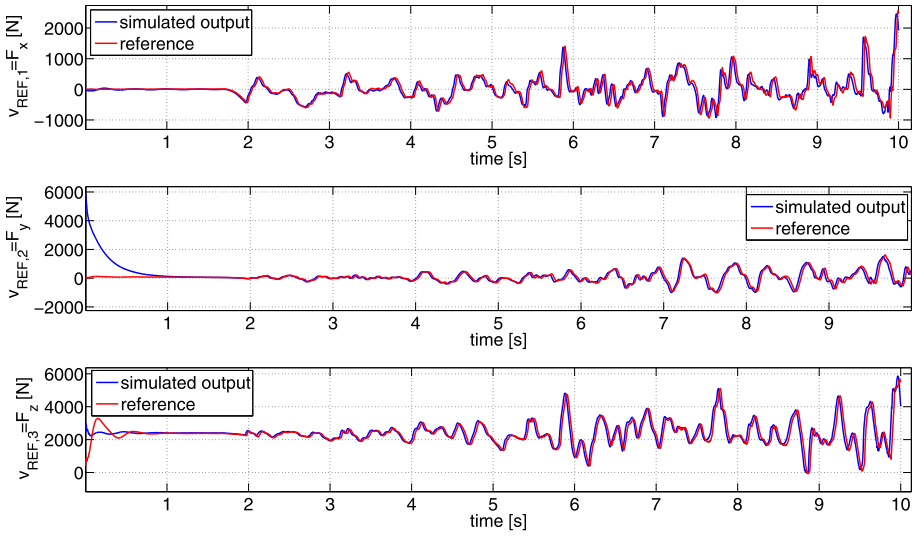

Fig. 6 Forces *front left*, VehicleVar1

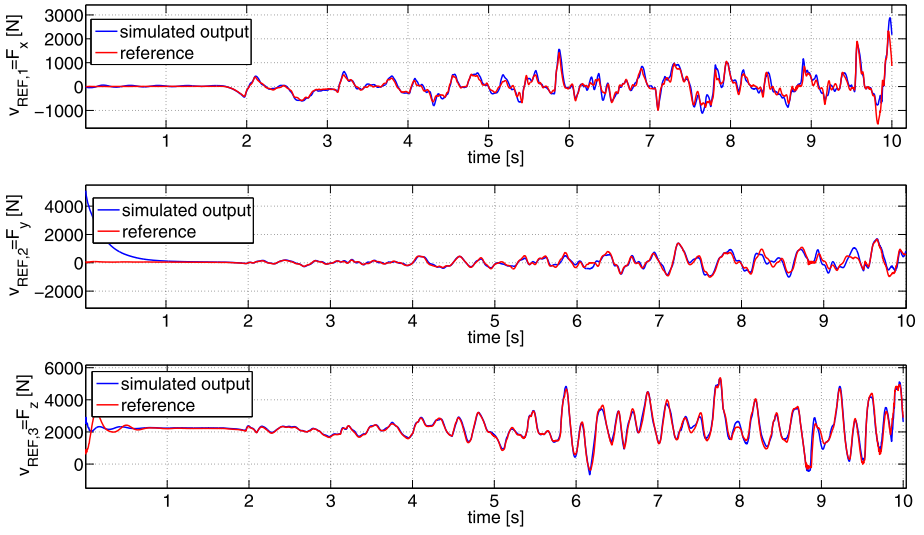

Fig. 7 Forces *front left*, VehicleVar2

and well acceptable quality, especially for VehicleVar1, which is also the vehicle variant closest to the original system A. This verifies that we have an input system that is invariant w.r.t. class $\mathcal{C}$ with a good quality. In the results for VehicleVar1, one can observe a small delay between the reference curve and the simulated one: this is due to the higher chassis mass, the controller in the virtual measurement simulation takes a bit longer to accelerate the heavier vehicle to the desired velocity. Nevertheless, apart from this delay, the curves

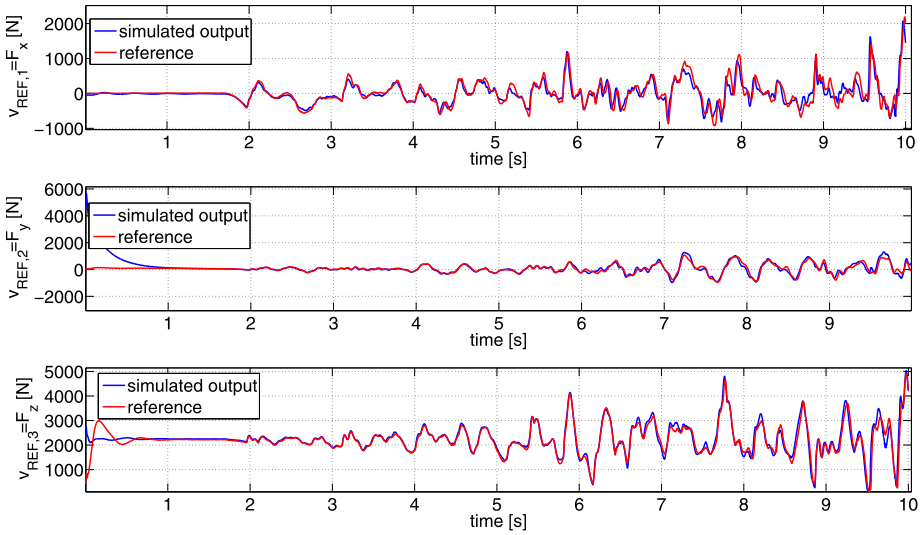

Fig. 8 Forces *front left*, VehicleVar3

characteristics coincide very well, which is important in vehicle engineering for durability purposes.

The goal of this simulation scenario was to check certain invariance properties of the proposed approach for a straight off-road drive. The obtained invariance results are very promising, and it can be expected that the approach produces results of similar quality for more complex variants.

If real measured reference signals are used, we can perform essentially the same steps. However, care should be taken in the ADAMS simulation of the reference system A, since we have to apply measured forces and torques as inputs for this simulation. To avoid the well-known drift-effect in such a scenario, cf. [27], one has to use a stabilization technique; for instance, one can use a measured motion of the vehicle's chassis to guide the vehicle during the simulation, [27]. For a full-vehicle simulation using our derived input systems, we do not need any stabilization technique. In addition, to ensure that the force-excited simulation is possible and produces reasonable results, the simulation model of the vehicle should be of a good quality, i.e., it should describe the vehicle, at which the spindle forces have been measured, sufficiently.

4 Conclusion

We have formulated an inverse control problem in terms of operator-theoretic concepts, the solution operator, and the input–output-operator. To solve the problem, we have presented and discussed the method of control constraints, which consists basically in solving an augmented DAE initial value problem. We have seen that this approach may suffer from a high index of the underlying DAE system, especially in case of an MBS, in which we have several bodies between the output and the body, at which the input acts. In practice, when large and complex simulation models are considered, this can lead to severe numerical problems,

i.e., order reduction and high sensitivity w.r.t. perturbations can occur during the numerical solution of the high-index DAE problem. Then index reduction may become inevitable. Nevertheless, for systems with low index, the method works well.

In Sect. 3, we have presented an approach to derive a virtual road profile as input for a tire-surrogate model based on measured spindle forces and an MBS model of the measurement vehicle which, however, should have a reasonable quality. To this end, we have solved an inverse control problem only for the tire-surrogate models with the method of control-constraints. This was possible with the help of a two-step procedure, and due to the specific interface between tire and vehicle model.

The virtual road profile together with the tire-surrogate model is considered as input data that possesses certain invariance properties and that can be used to simulate other vehicle variants. Indeed, a numerical simulation study underlines this property. We remark that the used tire-surrogate model is rather simple and of moderate complexity, which seems sufficient for the considered vehicle variants. We expect, however, an improvement of the invariance, i.e, the possibility to simulate variants with larger changes w.r.t. to the reference vehicle, when a more detailed, physical tire model is used.

Finally, we point out the flexibility and modularity of the approach proposed in Sect. 3. A change of the tire model only affects the solution of the inverse control problem. In addition, the vehicle MBS model, which might be complex and detailed, is always simulated within a state-of-the-art MBS software environment; the simulation is separated from the inverse problem, which can be solved by appropriate algorithms. This makes the approach applicable in industrial practice.

References

1. Adams, M.D.: MSC.Software GmbH, Am Moosfeld 13, 81829 Munich, Germany (2010)
2. Arnold, M., Burgermeister, B., Führer, C., Hippmann, G., Rill, G.: Numerical methods in vehicle system dynamics: state of the art and current developments. Veh. Syst. Dyn. **49**(7), 1159–1207 (2011)
3. Bäcker, M., Langthaler, T., Olbrich, M., Oppermann, H.: The hybrid road approach for durability loads prediction. SAE technical paper 2005-01-0628 (2005)
4. Blajer, W.: Dynamics and control of mechanical systems in partly specified motion. J. Franklin Inst. **334B**, 407–426 (1997)
5. Blajer, W., Dziewiecki, K., Kołodziejczyk, K., Mazur, Z.: Inverse dynamics of underactuated mechanical systems: a simple case study and experimental verification. Commun. Nonlinear Sci. Numer. Simul. **16**(5), 2265–2272 (2011)
6. Blajer, W., Kolodziejczyk, K.: A geometric approach to solving problems of control constraints: theory and a DAE framework. Multibody Syst. Dyn. **11**, 343–364 (2004)
7. Blajer, W., Kolodziejczyk, K.: Control of underactuated mechanical systems with servo-constraints. Nonlinear Dyn. **50**, 781–791 (2007)
8. Blajer, W., Kolodziejczyk, K.: Improved DAE formulation for inverse dynamics simulation of cranes. Multibody Syst. Dyn. **25**, 131–143 (2011)
9. Brenan, K.E.: Numerical solution of trajectory prescribed path control problems by the backward differentiation formulas. IEEE Trans. Autom. Control **AC-31**(3), 266–269 (1986)
10. Brenan, K.E., Campbell, S., Petzold, L.R.: Numerical Solution of Initial-Value Problems in Differential-Algebraic Equations. Classics in Applied Mathematics, vol. 14. SIAM, Philadelphia (1996)
11. Burger, M.: Optimal control of dynamical systems: calculating input data for multibody system simulation. Dissertation. TU Kaiserslautern (2011). Verlag Dr. Hut, München (2011)
12. Burger, M., Dressler, K., Speckert, M.: Invariant input loads for full vehicle multibody system simulation. In: Multiobody dynamics 2011 ECCOMAS thematic conference. Brussels and Fraunhofer ITWM Report 208 (2011)
13. Campbell, S., Gear, C.: The index of general nonlinear DAEs. Numer. Math. **72**, 173–196 (1995)
14. DeCuyper, J.: Advanced system identification methods for improved service load simulation on multi axial test rigs. Eur. J. Mech. Environ. Eng. **44**, 27–39 (1999)

15. DeCuyper, J.: Linear feedback control for durability test rigs in the automotive industry. PhD thesis, KU Leuven (2006)
16. Dressler, K., Speckert, M., Bitsch, G.: Virtual test rigs. In: Bottasso, C., Masarati Trainelli, P. (eds.) Multibody dynamics 2007, eccomas thematic conference, Milano, Italy (2007)
17. Eich-Soellner, E., Führer, C.: Numerical Methods in Multibody Dynamics. Teubner, Stuttgart (1998)
18. Fliess, M., Lévine, J., Martin, P., Rouchon, P.: Flatness and defect of non-linear systems: introductory theory and examples. Int. J. Control **61**(6), 1327–1361 (1995)
19. Gear, C.: Differential-algebraic equations, indices, and integral algebraic equations. SIAM J. Numer. Anal. **27**, 1527–1534 (1990)
20. Hairer, E., Lubich, C., Roche, M.: The Numerical Solution of Differential-Algebraic Systems by Runge-Kutta Methods. Lecture Notes in Mathematics, vol. 1409. Springer, Berlin (1989)
21. Hairer, E., Wanner, G.: Solving Ordinary Differential Equations II. Springer, Berlin (1996)
22. MathWorks: Matlab Version 7.80.347 (R2009a). http://www.mathworks.com
23. Rosen, A.: Applying the Lagrange method to solve problems of control constraints. J. Appl. Mech. **66**, 1013–1015 (1999)
24. Seifried, R.: Two approaches for feedforward control and optimal design of underactuated multibody systems. Multibody Syst. Dyn. **27**, 75–93 (2012)
25. Seifried, R., Blajer, W.: Analysis of servo-constraint problems for underactuated multibody systems. Mech. Sci. **4**, 113–129 (2013)
26. Sontag, E.D.: Mathematical Control Theory, 2nd edn. Springer, New York (1998)
27. Speckert, M., Ruf, N., Dressler, K.: Undesired drift of multibody models excited by measured accelerations or forces. J. Theor. Appl. Mech. **48**(3), 813–837 (2010)
28. Valášek, M.: Modelling, simulation and control of mechatronical systems. In: Arnold, M., Schiehlen, W. (eds.) Simulation Tecniques for Applied Dynamics. CISM Courses and Lectures, vol. 507, pp. 75–140. Springer, Berlin (2008)
29. Verwoerd, M.: Iterative Learning control—a critical review. Ph.D. thesis. Wöhrmann Print Service (2005)
30. Zilic, T., Kasac, J., Situm, Z., Essert, M.: Simultaneous stabilization and trajectory tracking of underactuated mechanical systems with included actuators dynamics. Multibody Syst. Dyn. **29**(1), 1–19 (2013)